Intravoxel incoherent motion (IVIM) and diffusion tensor imaging (DTI) in healthy kidney: Influence of renal flow challenge

E. E. Sigmund[1], P. H. Vivier[1], N. Lamparello[1], D. Sui[1], A. Mikheev[1], H. Rusinek[1], V. S. Lee[1], L. Zhang[1], and H. Chandarana[1]

[1]Radiology, New York University Langone Medical Center, New York, NY, United States

Background: Kidney diffusion-weighted imaging (DWI) has received considerable recent attention as protocols expand beyond an apparent diffusion coefficient (ADC) model, including (1) multiple b-values and intravoxel incoherent motion (IVIM) analysis to separate flow from parenchymal diffusion [1-4], and (2) multiple directions and diffusion tensor (DTI) analysis for diffusion anisotropy [5-7]. The former is thought to be sensitive to active vascular/tubular transport and the latter to static microstructure, but their full biophysical underpinnings or sensitivity to renal pathology (tubular necrosis, filtration deficit, rejection) are not yet established. Given the central role of tubular flow in renal filtration, we conducted normal control DWI evaluating two challenges that modify renal flow:(1) hydration, and (2) furosemide, to estimate sensitivity of advanced DWI to flow changes.

Methods: Using an IRB approved HIPAA compliant protocol, 10 volunteers were imaged in a Siemens full body Tim Trio 3 T with body and spine array coils. In one visit, subjects were scanned at baseline and after oral hydration (800 ml water over 60 min). In the second visit, subjects were scanned at baseline and after furosemide (20 mg IV injection). DWI used a twice-refocused spin echo sequence with bipolar diffusion gradients and coronal EPI readout.

IVIM: TR/TE= 850/76 ms, 156x192 matrix, interp. to 312x384, 1 slice, iPat=2, 2.1x2.1x6 mm voxel (interp. to 1x1 mm). Each of 3 breathholds included 8 b-values ($b=0,30,50,80,150,300,500,800$ s/mm^2), 3 directions, and 2 averages. Right kidney images were co-registered and averaged (Firevoxel software). Regions of interest (ROI) were placed on the b0 image on cortex (1 per slice) and medulla (~3/slice) and transferred to DWI to collect signal decay curves, which were analyzed by segmented biexponential curve-fitting (Igor Pro) [8]:

$$\frac{M}{M_0} = [(1-f_P)\cdot\exp(-b\cdot D_t) + f_P\cdot\exp(-b\cdot D_p)]$$

f_p is perfusion fraction, D_p is pseudodiffusivity and D_t is tissue diffusivity. Monoexponential fitting was performed to estimate apparent diffusion coefficient (ADC). Parametric maps were also generated. 1 case was discarded for poor image quality.

DTI: TR/TE=900/68 ms, 156x192 matrix, 3 slices, iPat=2, 2.1x2.1x6 mm voxel. Each of 3 breathholds included 2 b-values ($b=0,500$ s/mm^2), 6 directions (dual gradient scheme), and 3 averages. Right kidney images were co-registered and averaged using in-house software (Igor Pro), excluding misregistered or very low SNR images. DTI parametric maps were generated (Igor Pro) of mean diffusivity (MD), fractional anisotropy (FA), direction encoded colormap (DEC), and primary eigenvector. ROIs were placed on the b0 image on cortex (3 / case) and medulla (~9 / case) and transferred to the MD and FA maps. 3 cases were discarded for poor image quality.

Statistics: Means and standard deviations were calculated for all metrics (ADC, D_p, D_t, f_p, MD, FA). Student's two-tailed pairwise t-test was used to test reproducibility (baseline 1 vs. baseline 2) flow challenge (hydration/furosemide vs. average baseline BA) and tissue contrast (cortex vs. medulla). $p<0.05$ indicated significant differences.

Results: IVIM and DTI results from the same volunteer are shown in Figs. 1 and 2. IVIM ROI signals show biexponential decay. ADC, Dt, and MD parametric maps show some corticomedullary contrast (lower values in medulla). The FA map highlights medullary anisotropy, whose radial orientation is shown in diffusion eigenvectors. Figure 3 shows group averages from all diffusion metrics. The two baseline exams gave statistically equivalent results for all parameters. For all group means, Dt < MD < ADC. f_p and D_p values showed no significant differences between tissues and/or challenges. FA was significantly higher and MD significantly lower in the medulla than cortex for all scans except furosemide, where lower medulla MD was not significant. Medullary ADC was significantly lower than cortical ADC at baseline and furosemide. Hydration significantly increased cortical and medullary MD, Dt, and ADC, and decreased medullary FA. Furosemide significantly increased cortical and medullary Dt.

Discussion: The diffusion metrics considered here are differently sensitive to sampling and to physiological challenge. The hierarchy of "slow" diffusivities (Dt<MD<ADC) is driven by differential sampling of pseudodiffusion, maximally affecting ADC (all b-values), followed by MD (b = 0,500 s/mm^2), and minimally affecting Dt (b>200 s/mm^2). Corticomedullary differentiation was found in Dt, MD, and ADC, though not significantly for Dt, somewhat obscuring the flow/structure contributions. Hydration induced significant changes in MD, Dt, ADC, and FA values consistent with increases in isotropic "passive" diffusion such as higher fluid content or dilatation. The effect of furosemide was generally less pronounced than that of hydration. The "active" flow parameters fp and Dp showed no significant Cx/Md differentiation or challenge response, though trends of higher Dp with flow challenge bear further study. Though their values are robustly finite (Fig. 3) and accurate renal DWI requires flow consideration, the precise association of renal flow with apparent pseudodiffusion remains complex and may require novel physiological challenges or image analysis to resolve.
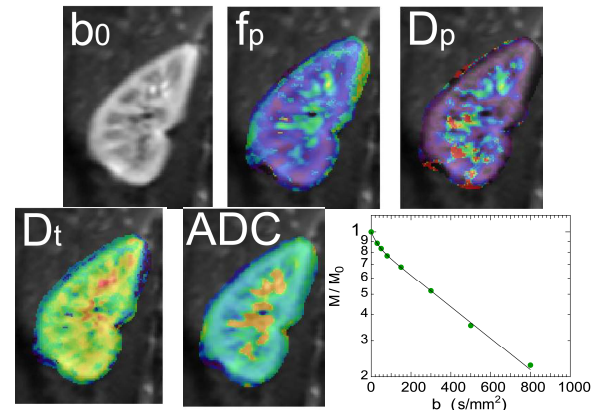

Figure 1: 3 T kidney IVIM in healthy volunteer. See Methods for image abbreviations. Lower right: Example cortex ROI signal decay and biexponential fit.
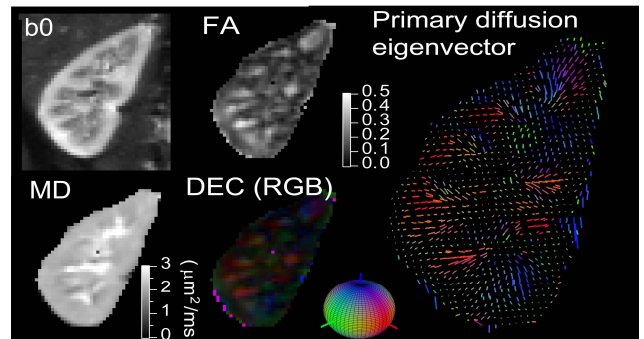

Figure 2: 3 T kidney DTI in healthy volunteer. See Methods for image abbreviations. Right panel: color-coded primary eigenvector map.
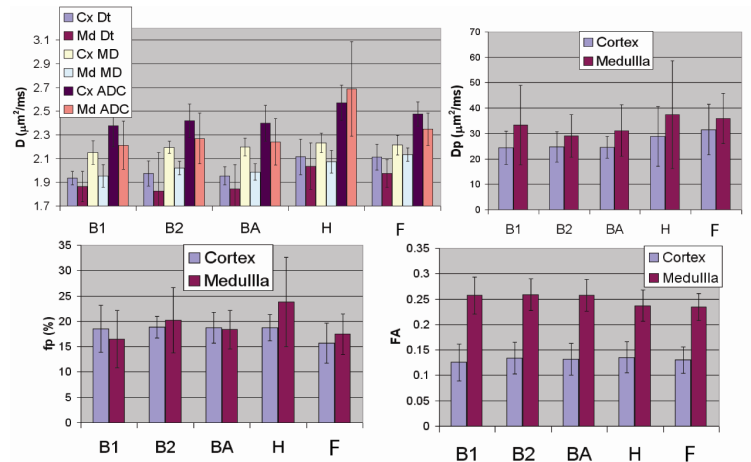

Fig. 3: Group averages. B1,2,A=baselines, H=hydration, F=furosemide.

References: 1.Thoeny HC, Radiology 2006;241(3):812-821. 2. Zhang J, ISMRM 2009 p 4111. 3. Yamada I, Radiology 1999;210(3):617-623. 4. Blinded. Radiology 2009;in press. 5. Ries M, JMRI 2001;14(1):42-49. 6. Notohamiprodjo M, Invest. Radiol. 2008;43(10):677-685. 7. Chandarana H, ISMRM 2009 p 405. 8. Lebihan D, Radiology 1988;168(2):497-505.